American Mineralogist, Volume 58, pages 850-868, 1973

Mössbauer Spectra of Synthetic Hedenbergite-ferrosilite Pyroxenes[1]

ERIC DOWTY[2]

U. S. Geological Survey, Washington, D. C.

D. H. LINDSLEY[3]

Carnegie Institution of Washington, Washington, D. C.

Abstract

The hedenbergite-ferrosilite series may be taken as representative in some respects of other sections across the common pyroxene quadrilateral. Data are reported for eight clinopyroxenes synthesized at a temperature above the augite-pigeonite solvus, plus two orthopyroxenes near ferrosilite in composition. Clinopyroxenes less calcic than about $Fs_{80}Wo_{20}$ were found to have the pigeonite structure ($P2_1/c$) on quenching.

The assignment of doublets and the interpretation of area ratios in the Mössbauer room-temperature spectra is clarified with the hypothesis that a distinct doublet arises from each of the four different types of next-nearest-neighbor configurations for iron cations in site $M1$. These four types arise from random distribution of calcium and iron in $M2$. Overlap of some of these doublets with the $M2$ doublet causes the area anomaly (overestimation of $M2$ area) previously noted when only two doublets are fitted. This overlap apparently also influences area ratios of liquid-nitrogen temperature spectra of high-calcium pyroxenes, but in these spectra, it does not seem to be possible to fit all the different $M1$ doublets, owing to their close superposition. This makes it questionable whether very accurate site distributions for high-calcium clinopyroxenes can be obtained from Mössbauer spectra, even at liquid-nitrogen temperature.

The quadrupole splitting of both M sites can be rationalized with Ingalls' crystal-field model. The $M1$ site, because of its low distortion, is very sensitive to small changes in its environment, hence the several doublets for different next-nearest-neighbor configurations. Variation in quadrupole splitting of the distorted $M2$ site, though less pronounced than that of $M1$, probably represents larger structural variations, because at high distortion, quadrupole splitting is less sensitive to small changes. The curve of $M2$ quadrupole splitting versus composition resembles in its shape the augite-pigeonite miscibility gap, providing a possible illustration of the crystal-chemical basis for this gap.

Introduction

The notorious complexity of the phase relations and crystal chemistry of the pyroxenes suggests that there may be a great deal of information about geologic processes in pyroxene assemblages. This complexity also makes it desirable to have information about pyroxene crystal chemistry and phase relations obtained with as many different experimental techniques as possible. We report here a reconnaissance study of a series of synthetic pyroxenes by Mössbauer resonance spectroscopy of iron.

The principal emphasis of most previous Mössbauer work on pyroxenes has been the measurement of order-disorder relations of iron and magnesium over the two nonequivalent metal sites, $M1$ and $M2$. For some compositions, order-disorder may be considered independently of the other problems of the crystal chemistry of pyroxenes. Study of this sort began with orthopyroxenes (space group *Pbca*), since they may be regarded as essentially a solid solution of enstatite ($MgSiO_3$) and ferrosilite ($FeSiO_3$). The first work was by X-ray diffraction

[1] Publication authorized by the Director, U.S. Geological Survey.

[2] Present address: Department of Geology and Institute of Meteoritics, The University of New Mexico, Albuquerque, New Mexico 87131.

[3] Present address: Department of Earth and Space Sciences, State University of New York, Stony Brook, New York 11790.

(Ghose, 1965), but emphasis has shifted where possible to Mössbauer spectroscopy because of greater precision and rapidity (*e.g.*, Virgo and Hafner, 1968, 1969, 1970; Dundon and Hafner, 1971; Saxena and Ghose, 1970, 1971).

Some work in the same vein has also been done on clinopyroxenes, augite (space group $C2/c$) and pigeonite ($P2_1/c$), especially since the return of the lunar samples (Bancroft and Burns, 1967a; Hafner and Virgo, 1970; Hafner *et al,* 1971). Interpretation of Mössbauer spectra of clinopyroxenes, however, is somewhat more complicated than that of orthopyroxenes, since clinopyroxenes often consist of an exsolution intergrowth of two phases. Clinopyroxenes also contain considerably more calcium than orthopyroxenes as well as somewhat larger quantities of minor elements such as aluminum, titanium and manganese. Also, certain technical points have not yet been established conclusively for clinopyroxene spectra, particularly the assignment of peaks and the relative rates of absorption, or recoil free fractions, of the two sites. One objective of the present study, concerned with a series of magnesium-free pyroxenes on the join hedenbergite ($CaFeSi_2O_6$)-ferrosilite ($FeSiO_3$), was to provide some background for general clinopyroxene study in the form of assignment of peaks in the spectra, and interpretation of the area ratios of the peaks for the two sites. A second objective was to try to provide some crystal chemical information which might not be obtainable with other methods, through study of the hyperfine parameters, quadrupole splitting, and isomer shift.

The choice of the join hedenbergite-ferrosilite over similar but more magnesian sections in the pyroxene quadrilateral (diopside-hedenbergite-ferrosilite-enstatite) is advantageous for several reasons. First, subsolidus phase relations on this join are comparatively well known, whereas little work has been done in the interior of the pyroxene quadrilateral. Second, restriction to two kinds of cations, Fe and Ca, reduces ambiguity in the interpretation of Mössbauer area ratios. Third, the relatively high iron content facilitates Mössbauer study. Our pyroxenes were all made at 20 kbar, not because we wanted to study high-pressure phases, but because this suppresses fields of pyroxenoid and of fayalite plus silica, which would have interfered with synthesis of a complete series of pyroxenes at lower pressure. In respect to many of the crystal-chemical properties here of interest, the hedenbergite-ferrosilite join at 20 kbar should be representative of more magnesian sections of the pyroxene quadrilateral at lower pressures.

A room-temperature Mössbauer study of a series of clinopyroxenes on the join hedenbergite-ferrosilite was reported by Dundon and Lindsley (1967), and preliminary results for the present study at liquid nitrogen temperature (90°K) were given by Dowty and Lindsley (1970). More extensive work, including particularly room temperature spectra, has shown that some suggestions made in the latter report were probably unwarranted; this report should be considered as superseding the earlier work.

Experimental

Synthesis

Pyroxenes used in this study were synthesized from mixtures of Fe-sponge, Fe_2O_3, quartz (from Lisbon, Maryland) or SiO_2-glass, and (except for pure $FeSiO_3$) $CaSiO_3$ previously made from $CaCO_3$ and quartz. (Details of the starting chemicals and weighing procedure have been given by Lindsley and Munoz, 1969, p. 320). In most cases these starting materials were initially reacted in evacuated silica-glass tubes at 900–950°C to mixtures of fayalitic olivine, silica, and (for all but the most iron-rich compositions) calcium-rich metasilicate. Approximately 0.7 g of the pre-reacted mixes were then sealed into silver capsules (12.7 mm long by 6.35 mm outer diameter) together with 20 mg distilled H_2O, and 1 to 2 mg excess silica glass to saturate the vapor phase. Initial attempts to synthesize iron-rich pyroxenes yielded products with several percent magnetite, presumably caused by the diffusion of hydrogen through the silver capsules. Addition of trace amounts of acetone to the starting materials inhibited this oxidation. Each capsule was then reacted for approximately 2 hours at 20 kbar and 950°C in piston-and-cylinder apparatus. Two of the pyroxenes, $Fs_{87.5}$ and Fs_{100}, were synthesized by repeated runs in smaller (~0.01 g capacity) capsules.

Other than pyroxene, the run products were primarily fayalite and silica, and occasionally very minor amounts of magnetite. Products were ground and rerun until the content of unreacted fayalite plus silica was judged by microscope examination to be well under 1 per cent. Microprobe examination of pyroxenes synthesized under similar conditions has shown that compositional variations are less than

3 per cent $CaSiO_3$. Incomplete reaction would tend to make the pyroxenes slightly more calcic than their nominal composition, but the average composition is probably within one-half percent of the nominal value.

Mössbauer

Samples were fine-ground and mounted in one-inch diameter disks of Buehler transoptic plastic. Spectra were taken on a 200 channel, constant-acceleration "flyback" spectrometer (DeVoe, 1967). Velocity increment per channel was usually about 0.04 mm/sec. Concentrations of iron in the absorbers and background counts recorded for each spectrum are given in Tables 3 and 8. The resonance effect at the peaks assigned to the $M1$ doublet was in the neighborhood of 10 to 12 percent at liquid nitrogen temperature for the absorbers with the greatest concentration of iron, and correspondingly less for those with smaller concentrations. A metallic iron foil with concentration 18 mg/cm^2 of natural iron was used for calibration. All I.S. (isomer shift) values are reported relative to iron = 0.0 mm/sec. Liquid-nitrogen temperature spectra were taken in moving-source geometry in a styrofoam-insulated cryostat (DeVoe, 1967), using a source consisting of Co^{57} in metallic chromium; the source was at room temperature. The widths of the inner two lines of the metallic iron calibration spectrum measured at room temperature were 0.30 mm/sec with this source and geometry. Absorber temperature in the liquid-nitrogen cryostat is assumed to be 90°K (DeVoe, 1967). Room temperature (294K ±1°) spectra were taken in moving absorber geometry, using a source of Co^{57} in metallic palladium. With this source the widths of the inner two lines of the iron spectrum were 0.25 mm/sec.

Theoretical line shapes were fitted to the data with a Fortran program on the IBM 360/65 computer, using an adaptation of the metric minimization procedure of Davidon (1959). Chi-square, the usual residual, was minimized.

Ideally, line shapes are given by the Lorentzian formula, in which the absorption at each channel due to each peak is given by

$$f(x) = \frac{2A}{\pi\Gamma\left\{1 + 4\left(\frac{x - x_o}{\Gamma}\right)^2\right\}}$$

where x is channel number, A is the area, x_0 is the location in channel number of the peak, and Γ is the full width at half height. However, experimental lines are usually more or less nonideal. In fitting the synthetic pyroxenes, a Gaussian component was added in some cases, in order to take better account of several types of nonideality of line shape. Line broadening caused by essentially random factors, such as inhomogeneities in composition, chemical disorder over some sites, temperature variations, crystalline defects, *etc,* should lead to a Gaussian "smearing" of the line. The true line shape in this case would probably be closely approximated by a combination of Gaussian and Lorentzian shapes. A line shape of this kind, called the Voigt profile, is well known in spectroscopy (see, for example, Posener, 1959). An exact evaluation of this line shape calls for solving an integral at each wavelength or data point. We have not yet been able to adapt an accurate method for approximating the integral to rapid least-squares analysis, and we have therefore adopted a simple sum of Lorentzian and Gaussian terms to describe the line shape. The line shape we used for the final fits, following suggestions by W. A. Dollase (personal communication) is:

$$g(x) = \frac{2A}{\Gamma}\left[\frac{1 - \alpha}{\pi\left\{1 + 4\left(\frac{x - x_o}{\Gamma}\right)^2\right\}} + \alpha\sqrt{\frac{\ln 2}{\pi}}\exp\left\{-4\ln 2\left(\frac{x - x_o}{\Gamma}\right)^2\right\}\right] \quad (1)$$

where α is the fraction of the area accounted for by the Gaussian part of the line. There are thus four parameters to be simultaneously varied for each peak, A, x_o, Γ and α, instead of three as in the case of pure Lorentzian lines.

Such a line shape is only an approximation, but it has been found to be very useful with respect to reducing the residual chi-square, and it is doubtful if a more accurate approximation is justifiable in many cases of mineralogical Mössbauer spectroscopy. We did attempt to approximate the integral (Voigt profile) numerically by means of a small (5 to 7) number of Lorentzian peaks having a Gaussian distribution, but the computing time was increased, while the residual was not significantly reduced compared to the fits using the line shape given in equation (1) above.

Almost invariably, the use of the partially Gaussian line shape has been found to reduce the residual of fits in far greater proportion than would be ex-

pected solely from the additional adjustment parameter. In many spectra of chemically complex or inhomogeneous compounds, there is a particular kind of "misfit" when Lorentzian lines are assumed—the fit generally overestimates the absorption in the region of the tails and at the precise center of the peak, while it underestimates the absorption just to either side of the peak center. This kind of misfit is "cured" when a Gaussian term is added.

There are real dangers, however, in the use of the Gaussian term. The principal one seems to be that it also reduces the residual when *non*-random deviations from Lorentzian shape are involved. The present work gives an example of a case in which several distinct, non-randomly distributed peaks appear to be a more correct description of the spectra than single Lorentzian or partially Gaussian lines.

Errors of Mössbauer Measurements

The estimated standard deviations for the parameters derived from our least-squares fits are given in parentheses in the tables. Some cautionary words about these errors are in order, however. They apply for the most part only to the lack of precision introduced by counting statistics in each spectrum (and also in the calibration spectrum, in the case of hyperfine parameters and widths). It is unlikely, for example, that errors introduced by velocity drift in the spectrometer and other instrumental errors are fully accounted for, and of course, error in composition introduced during synthesis is not considered at all. Also, the errors apply only to the particular parameter space assumed for the fit, that is, if different numbers of peaks are assumed, very different parameters with non-overlapping errors are obtained. A special case occurs when the number of parameters is almost equal to the number of channels which give useful information; at this point, the assumptions which underlie the derivation of errors from least squares fits begin to break down. We may be approaching this case in the multi-doublet fits to room-temperature spectra discussed below.

Without extensive replication of all steps in the experiment, including synthesis, absorber preparation, and sample and calibration spectral runs, an accurate estimate of the precision is impossible. We believe, however, that the hyperfine parameters and widths are reproducible to about 0.02 mm/sec, and the fractional areas to about 0.01 to 0.02 for simpler spectral models, *i.e.*, one $M1$ and one $M2$ doublet, and perhaps two to three times these values for the multi-doublet models.

Phase Composition of the Pyroxenes

Since exsolution and domain structures are common in clinopyroxenes, we have tried to characterize the material closely insofar as possible by single-crystal X-ray study. C. W. Burnham and Y. Ohashi, who are presently carrying out independent diffraction investigations of some of the material synthesized in this and previous studies, have supplemented our results in this respect.

Ten pyroxenes (Table 1) were synthesized at 950° C and 20 kbar. Although there is a change of symmetry in the series, from $C2/c$ (diopside or hedenbergite structure) in the more calcic compositions to $P2_1/c$ (clino-enstatite or pigeonite structure) in the less calcic ones, no definite evidence was found for the existence of an augite-pigeonite solvus. X-ray powder photographs, taken on the Hägg-Guinier camera, and powder diffractograms of the composition in the critical region $Fs_{70}Wo_{30}$ to $Fs_{90}Wo_{10}$, showed no splitting of lines which could be ascribed to the presence of two pyroxenes. Some of the lines were fairly broad, but this was characteristic of most specimens and can probably be ascribed to the compositional inhomogeneities of 3 percent or less expected in such syntheses (see above). These findings are consistent with the hypothesis of Lindsley and Munoz (1969) that the clinopyroxene solvus on this join is occluded metastably within the orthopyroxene-clinopyroxene field at temperatures below 950°C. The previous finding that $P2_1/c$ pyroxenes invert to $C2/c$ at high tem-

TABLE 1. Symmetries of Synthetic Pyroxenes

Fs Content	Optical symmetry	X-ray space group	X-ray method
50	monoclinic	–	–
60	"	–	–
70	"	–	–
75	"	C2/c	precession
80	"	2 crystals C2/c 2 crystals $P2_1/c$*	precession (4 crystals)
85	"	$P2_1/c$**	precession
87.5	"	$P2_1/c$	precession
90	"	$P2_1/c$	Guinier
98	orthorhombic	–	–
100	"	–	–

*Y. Ohashi, personal communication. The crystals of $Fs_{80}Wo_{20}$ were taken from a special run made for the sole purpose of obtaining large crystals. The charge was seeded with several crystals from a previous run. The large crystals thus obtained might be expected to be somewhat inhomogeneous, and the presence of both symmetries does not necessarily indicate the existence of a two-clinopyroxene field at the nominal composition.

**C.W. Burnham, personal communication.

peratures (Smyth, 1969) suggests that the less calcic clinopyroxenes may actually have formed with $C2/c$ symmetry, as part of a complete clinopyroxene series, and that they inverted to $P2_1/c$ on cooling.

A domain structure of some $P2_1/c$ pyroxenes has been inferred from the diffuseness of the $h + k$ odd reflections (Morimoto and Tokonami, 1969; Clark *et al,* 1971), and corresponding domain boundaries have been observed in electron micrographs (*e.g.,* Christie *et al,* 1971). None of our $P2_1/c$ pyroxenes which had grains large enough for single-crystal study appeared to have diffuse $h + k$ odd reflections (Y. Ohashi, personal communication). There is hence no evidence for Morimoto-type domains.

Thus all our pyroxenes seem to be single-phase specimens, with no exsolution, and no apparent domain structure. It is important to point out, however, that most of these compositions are only stable at high temperature, and those within the broad orthopyroxene-clinopyroxene solubility gap found by Lindsley and Munoz (1969) are metastable at room temperature with respect to two pyroxenes. (Of course, at low pressure the more iron rich ones are also metastable with respect to fayalite plus quartz.)

Assignment and Area Ratios of Mössbauer Peaks

Room Temperature Spectra

In the pyroxene structure, there are two metal sites, $M1$ and $M2$. $M1$ is occupied in both hedenbergite and ferrosilite by ferrous iron, while $M2$ is occupied in hedenbergite by calcium, and in ferrosilite by ferrous iron. Ferrous iron in each of these sites would normally be expected to give rise to a doublet, and often two apparent doublets can be distinguished by eye in the spectra. In orthopyroxenes, the two outer peaks have been assigned to iron in $M1$, and the two inner peaks to iron in $M2$. We have found this assignment to be correct also for the hedenbergite-ferrosilite series at both room and liquid-nitrogen temperatures. Recent work (Williams *et al,* 1971) has also confirmed this assignment for certain natural sub-calcic pyroxenes.

However, in previous work and the present study, anomalies have been found in the relative areas of the peaks in room temperature spectra of some clinopyroxenes when the above assignment is followed. Often, one or both of the peaks for $M2$ seem far too intense. This is one reason why alternate assignment schemes have been proposed for some clinopyroxenes (Bancroft, Maddock, and Burns, 1967; Dundon and Lindsley, 1967; Matsui, Maeda, and Syono, 1970). Williams *et al* (1971) found these anomalies to be generally present in natural and synthetic $C2/c$ pyroxenes, and attempted to explain them by postulating a domain structure whereby two distinct phases, differing primarily in calcium content, and therefore two doublets for each site would be expected. They suggested that the $M2$ doublets for the two phases were essentially coincident, while the $M1$ doublets were separated at room temperature. If one of the $M1$ doublets were close to the $M2$ doublets, fitting only two doublets to the spectrum might tend to augment the area of the $M2$ doublets at the expense of $M1$. Williams *et al* (1971) were able to obtain $M1/M2$ area ratios which agree with those from the liquid-nitrogen temperature spectra by fitting *two* $M1$ doublets. At liquid nitrogen temperature, according to this hypothesis, the $M1$ doublets become more similar to each other, while both are resolved more distinctly from the $M2$ absorption.

Like Williams *et al* (1971), we suppose that more than one doublet is necessary to describe the $M1$ absorption. However, we propose an explanation for this which is somewhat different and more satisfactory in certain respects than the domain hypothesis. Our hypothesis involves variation in *next-nearest-neighbor* configurations of the $M1$ site, due to purely random distribution of iron and calcium in the $M2$ site. Although next-nearest-neighbor influence has been considered as a cause of variation of hyperfine parameters in silicates (Bancroft, Maddock, and Burns, 1967), it has not generally been thought to be sufficient to cause actual splitting of the doublets. However, it will be shown in the next section that quadrupole splitting of iron in the pyroxene $M1$ site, because of the low distortion of this site, is extraordinarily sensitive to small changes in the environment, more so than iron in most silicate sites.

Each $M1$ octahedron in pyroxene shares edges with three $M2$ polyhedra. As the composition changes through the series hedenbergite-ferrosilite, the occupancy of the $M2$ site changes from all calcium to all iron. The $M1$ octahedron also shares edges with other $M1$ octahedra, but $M1$ is always occupied by iron. Thus, four basically different types of next-nearest-neighbor configuration may be distinguished for the $M1$ site, according to whether the three adjacent $M2$ sites are occupied by: (1) three iron atoms; (2) two iron atoms and one calcium atom;

(3) one iron atom and two calcium atoms; and (4) three calcium atoms. The probabilities of each of these configurations, assuming random distribution of cations in *M*2, are easily worked out for each composition, and the resultant expected fractional areas, with the expected fractional area of the *M*2 site, are shown in Table 2.

The *M*2 polyhedra share corners, but not edges, with other *M*2 polyhedra. Furthermore, as will be shown in the next section, quadrupole splitting of the *M*2 site is not nearly so sensitive to small changes in the environment as that of *M*1. Therefore, only a single doublet is expected for *M*2.

In attempting to fit theoretical line shapes to the room temperature spectra, we have considered four hypotheses: (1) that the absorption for each site consists of a single doublet, with lines of Lorentzian or near Lorentzian shape; (2) that each site is represented by a doublet with lines of partially Gaussian shape, that is, lines which have been broadened by essentially random factors; (3) that the *M*2 absorption is adequately represented by a single doublet, but that the *M*1 absorption is split into two doublets because of the presence of domains as suggested by Williams *et al* (1971); (4) that the *M*2 absorption is adequately represented by one doublet, but that the *M*1 absorption is split into up to four doublets, because of next-nearest-neighbor effects, as explained above. Chi-square values for the four types of fit are given in Table 3.

(1) When four Lorentzian lines (two doublets) were fitted, with no constraints, the *M*2/*M*1 area ratios obtained were anomalous—the *M*2 area was larger than predicted, and this anomaly increased with calcium content (Table 4). Our spectra are very similar in this respect to those of Dundon and Lindsley (1967), provided we assign their peaks so that the *M*2 doublet is inside the *M*1 doublet. These area ratios are quite unacceptable, and indicate that this description of the spectrum is inadequate. Furthermore, values of chi-square for these fits are very high (Table 3).

(2) Addition of a Gaussian component to the fitted lines reduced chi-square values, but the anomalies in area ratios persisted (Table 4). We tentatively conclude from this that the perturbing influences on the *M*1 doublet are not random.

(3) Several attempts to fit two *M*1 doublets and one *M*2 doublet were unsuccessful with respect to obtaining reasonable and systematic area ratios, quadrupole splitting, and isomer shift, although chi-square was usually reduced in these fits (Table 3). When the peaks were unconstrained (using either pure Lorentzian or partially Gaussian lines), match-ups of peaks into doublets were not obvious from their areas, and if peaks were assigned to doublets on the basis of the conventional assignment, which assumes the two *M*1 doublets to have similar isomer shifts, no systematic patterns were discerned in the relative areas of the two *M*1 doublets. Also, for many of the spectra, the resultant *M*2/*M*1 area ratios did not agree well with those expected. Fits were tried with heights and widths of the two peaks of each doublet constrained to be equal, but in this case, the locations of the *M*1 peaks sometimes migrated in such a way that the isomer shifts of the two *M*1 doublets were not nearly the same (in other words, the locations of two of the *M*1 peaks which were close together would be interchanged).

TABLE 2. Expected Relative Iron Occupancies for the *M*2 Site and Four Next-Nearest-Neighbor Configurations of the *M*1 Site in Hedenbergite-Ferrosilite Pyroxenes

Fs Content	M1* (1) 3Fe,0Ca	(2) 2Fe,1Ca	(3) 1Fe,2Ca	(4) 0Fe,3Ca	M2
50	-	-	-	1.0	-
60	0.007	0.080	0.320	.427	0.167
70	.046	.206	.308	.154	.286
75	.083	.250	.250	.083	.333
80	.135	.270	.180	.040	.375
85	.202	.259	.111	.016	.412
87.5	.241	.241	.080	.009	.429
90	.285	.214	.053	.004	.444
98	.451	.056	.002	-	.490
100	.500	-	-	-	.500

*Divided according to the occupancy of the three adjacent M2 sites. Probabilities for the different configurations are computed as follows: $P(1) = x^3$, $P(2) = 3x^2y$, $P(3) = 3xy^2$ and $P(4) = y^3$, where P(i) is the probability for the i'th configuration as given at the head of the table, and x and y are the fraction of iron and calcium, respectively, in M2. These probabilities are then multiplied by the total fraction of iron in M1, in order to get relative areas.

TABLE 3. Data Collection Information and Chi-Square Values for Room Temperature Spectra of Synthetic Hedenbergite-Ferrosilite Pyroxenes

Fs Content	Iron conc. mg/cm^2	Bkgd. cts. x 10^5	Chi-square 2-doub. Lorent.	2-doub. Gauss.	3-doub. Lorent.	n-doub. Lorent.	n
50	3.7	3.8	177	174	-	-	2
60	4.6	5.6	388	208	210	179	4
70	3.8	6.9	311	153	139	157	4
75	7.0	5.4	237	155	116	127	5
80	7.3	5.7	639	235	234	192	4
85	6.7	5.7	563	204	300	250	4
87.5	2.6	6.5	135	103	121	127	4
90	8.7	5.6	448	235	252	349	3
98	7.9	5.8	237	173	176	-	2
100	3.2	7.5	149	141	-	-	2

TABLE 4. Area Ratios and Mössbauer Parameters (mm/sec) for Two-Doublet Fits to Room Temperature Spectra of Synthetic Hedenbergite-Ferrosilite Pyroxenes

Fs Content	M2 Area Expected	M2 Area Lorent.	M2 Area Gauss.	M1 QS	M1 IS	M1 Widths L	M1 Widths H	M2 QS	M2 IS	M2 Widths L	M2 Widths H
50	0.0	--	--	2.222(2)	1.188(2)	0.294(5)	0.297(5)	--	--	--	--
60	.167	0.436(17)	0.251(3)	2.360(5)	1.187(2)	.477(11)	.476(8)	1.909(10)	1.138(5)	0.349(13)	0.412(9)
70	.286	.455(7)	.473(9)	2.573(7)	1.183(4)	.408(11)	.395(7)	1.862(7)	1.140(4)	.332(11)	.422(6)
75	.333	.466(15)	.512(9)	2.570(6)	1.163(3)	.338(12)	.392(6)	1.823(7)	1.105(4)	.369(9)	.375(6)
80	.375	.456(7)	.496(4)	2.545(3)	1.177(2)	.359(7)	.394(5)	1.763(3)	1.116(2)	.322(6)	.372(5)
85	.412	.512(7)	.537(3)	2.520(3)	1.180(2)	.339(5)	.356(5)	1.798(3)	1.114(2)	.326(4)	.396(5)
87.5	.429	.509(11)	.516(4)	2.538(7)	1.169(3)	.334(6)	.348(5)	1.844(6)	1.117(3)	.330(6)	.365(6)
90	.444	.523(8)	.545(4)	2.547(3)	1.176(2)	.321(5)	.323(4)	1.887(3)	1.125(2)	.315(4)	.376(6)
98	.490	.480(8)	.478(3)	2.488(3)	1.179(1)	.313(4)	.285(4)	1.910(3)	1.125(2)	.281(4)	.289(4)
100	.500	.457(9)	.434(8)	2.490(5)	1.182(3)	.296(10)	.264(6)	1.906(4)	1.130(2)	.256(9)	.236(5)

Quadrupole splitting (QS), isomer shift (IS), and full widths at half-height (low and high velocity) are from partially Gaussian fits. Figures in parentheses represent estimated standard deviation from the least-squares fits, in terms of the least units cited.

Of course, we cannot claim to have exhausted all the possibilities for starting parameters in this type of fit, and the experiment is not completely conclusive for this reason. The domain hypothesis at present does not furnish *a priori* prediction of relative areas of the two *M*1 doublets or their parameters, so that there is no other way than trial and error to try to fit doublets in this hypothesis.

(4) In fitting multiple doublets according to the next-nearest-neighbor hypothesis, starting peak parameters were derived using the predicted areas given in Table 2, and it was assumed that the several *M*1 doublets for each spectrum had nearly the same isomer shift. A next-nearest-neighbor configuration was neglected if its predicted area was less than 6 percent of the total absorption. Pure Lorentzian line shapes were used, and both heights and widths of the two peaks of each doublet were constrained to be equal, in order to keep to a minimum the number of variable parameters. Some representative spectra are shown in Figure 1.

The results of this process appeared to be satisfactory, keeping in mind the limitations of the data. The line widths and isomer shifts were reasonable, and the quadrupole splitting for the various *M*1 configurations fell into a remarkably consistent pattern (Tables 6 and 7, Figure 5). Some of these aspects will be discussed in more detail below. Chi-square for these fits was as low as that for any of the other types of fits (Table 3). Final fractional areas were in most cases within a few percent of the predicted values (Table 5). Better agreement is hardly to be expected, considering that as much as 6 percent of the predicted area was deliberately neglected in some cases, and that the heights and widths were constrained. Also, although only four configurations are shown in Table 2, the middle two could be broken down even further, according to which of the adjacent *M*2 polyhedra, only two of which are equivalent to each other by the point symmetry of the *M*1 site, is occupied by the single iron or calcium atom.

Of course, we cannot claim that these are the only correct or the optimum doublets which could be fitted to the data. The number of data points in each spectrum which actually give useful information is small enough, and the number of fitted parameters is large enough, so that fitting this many doublets is probably near marginal in a purely statistical sense. However, the limits of the particular data used in this case, and of the technique in general, must be accepted. It might be possible to obtain a statistically more valid test of the hypothesis by taking spectra with more channels for much longer counting times, but we suspect that with the peaks being as close together as postulated, the limit of instrumental resolution would be reached before a statistically valid distinction between hypotheses (3) and (4) could be made.

The next-nearest-neighbor hypothesis is so far consistent with all observations, but the same cannot be said of any of the other three hypotheses considered above. The first two hypotheses can be ruled out because they give unsatisfactory area ratios. The domain hypothesis appears to have several serious deficiencies. (a) Although some satisfactory area ratios (satisfactory by comparison with liquid-nitrogen temperature spectra) and hyperfine parameters were obtained for some natural and synthetic pyroxenes (Williams *et al*, 1971), we have been unable to obtain confirmation of reasonable area ratios and Mössbauer parameters for the heden-

bergite-ferrosilite series. (b) If a domain structure actually existed in $C2/c$ pyroxenes, we would expect its detection in at least some specimens by other techniques. However, there have been no reports of detection of domain structure in $C2/c$ pyroxenes by X-ray or electron diffraction, or electron microscopy. (c) The fact that the pyroxenes which are supposed to have domain structure give normal, sharp diffraction photographs puts very severe limitations on the nature of the domains. In the $C2/c$ pyroxenes, this requires either that one of the two types has individual domains so small that its diffraction effects are too diffuse to be observed, or that the two types have exactly the same symmetry and lattice constants —otherwise we would see two diffraction patterns. The first alternative implies that the relative volume of the type with small individual domains should also be small in relation to the volume of the other type, barring a rather peculiar and unlikely size distribution of domains. However, the results of Williams *et al* (1971) in some cases show comparable areas for the doublets attributed to the two types of "domains", which seems to rule out this alternative. The second alternative implies, in effect, a miscibility gap *within* the $C2/c$ field, and we would therefore predict that some $C2/c$ pyroxenes, those lying outside the gap, would have no domain structure and no area anomaly. All of our $C2/c$ pyroxenes show an area anomaly. Furthermore, our $P2_1/c$ pyroxenes also show area anomalies, which would seem to require a different type of domain structure.

Liquid-nitrogen temperature spectra

In liquid-nitrogen temperature spectra, the $M1$ peaks become more clearly separated from the $M2$ peaks, because of a greater increase of $M1$ quadrupole splitting with decreasing temperature (see below). At the same time, it must be presumed that the doublets for the various $M1$ configurations become more alike, because in two-doublet fits, the area ratios are much closer to the predicted values (Table 9, Figure 7). This is presumed in the domain hypothesis (Williams *et al,* 1971) as well as in the next-nearest-neighbor hypothesis. A probable reason for the greater similarity of the $M1$ doublets at low temperature will be discussed in the next section.

We were not successful in attempting to fit multiple $M1$ doublets to the liquid-nitrogen temperature spectra. The final relative areas of the various $M1$ doublets for such fits appeared to be essentially random. The result was the same when only two doublets (domain hypothesis) were tried. This is not surprising if we consider that the $M1$ doublets are very nearly superimposed. The information in the spectra useful for fitting more than one $M1$ doublet would be even less than in the room temperature

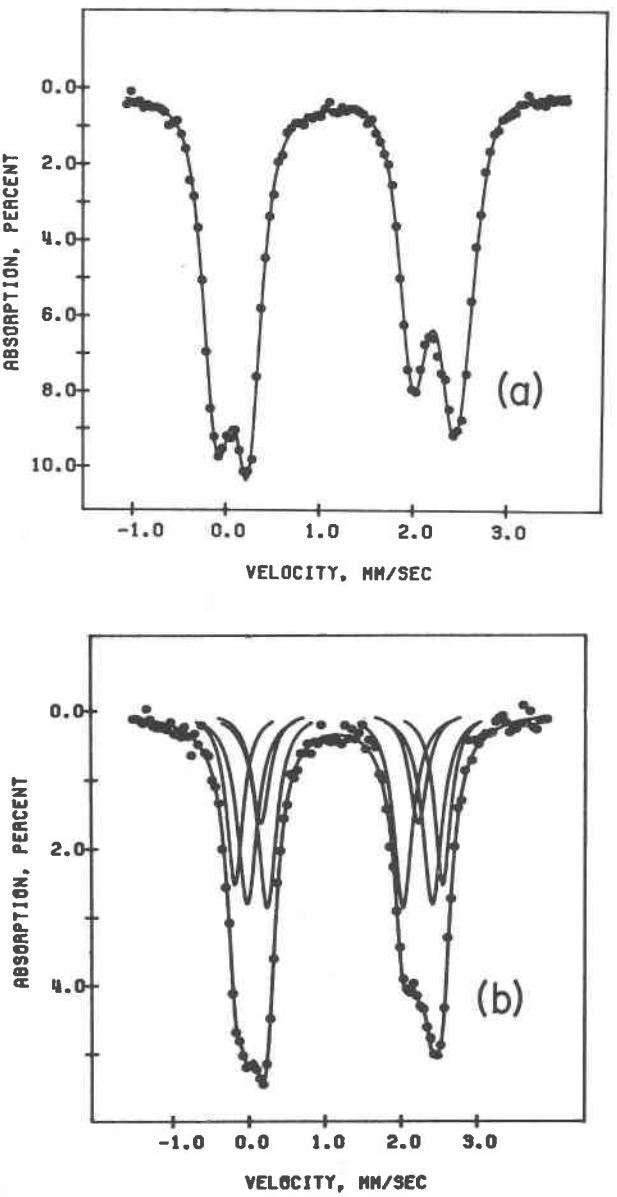

FIG. 1. (a) Room temperature spectrum of $Fs_{80}Wo_{20}$, fitted with two partially Gaussian doublets. The fit is visually good, but gives an $M2$ relative area that is about 20 percent too high.

(b) Room temperature spectrum of $Fs_{70}Wo_{30}$, fitted with one $M2$ and three $M1$ doublets. From center outward in either direction, the peaks are assigned to: $M2$, $M1(4)$, $M1(3)$, and $M1(2)$ (see Table 2).

TABLE 5. Measured Relative Areas for Multi-Doublet Fits to Room Temperature Spectra of Synthetic Hedenbergite-Ferrosilite Pyroxenes

Fs Content	M1 * (1)	(2)	(3)	(4)	M2
50	-	-	-	1.000	-
60	-	0.051(1)	0.314(3)	.436(2)	0.200(2)
70	-	.228(1)	.308(2)	.162(1)	.302(2)
75	0.0783(6)	.247(2)	.263(2)	.083(6)	.331(2)
80	.1129(8)	.328(2)	.194(1)	-	.366(2)
85	.170(1)	.214(2)	.179(1)	-	.436(2)
87.5	.267(2)	.273(2)	.0808(6)	-	.380(2)
90	.270(2)	.294(2)	-	-	.436(2)
98	.520(8)**	-	-	-	.480(8)**
100	.543(9)**	-	-	-	.457(9)**

*Divided as in Table 2.

**Values from Table 4.

Figures in parentheses represent estimated standard deviation from the least-squares fits, interms of least units cited.

spectra, and the operation is certainly unjustifiable statistically.

Although the area ratios for two-doublet liquid-nitrogen temperature fits are much improved over those for room temperature, there is still a significant difference between measured and predicted values (Fig. 7). We have taken our "final" area ratios for liquid-nitrogen spectra from partially Gaussian fits, which give much lower values of chi-square than pure Lorentzian fits. The area ratio anomaly usually seems slightly less for pure Lorentzian fits, but is nevertheless significant at all compositions. Thus, there is clearly a bias with respect to $M1/M2$ area ratios in our spectra, at liquid nitrogen temperature. It seems most reasonable to suppose that the cause of the bias is the same as that for room-temperature spectra, namely, overlap due to splitting of $M1$ absorption. Indeed, it would be fortuitous if such a cause were present at room temperature but completely absent at liquid-nitrogen temperature. However, in view of the practical implications of such a cause of bias on the measurements of cation distribution, a discussion of certain alternate possible causes of the bias at liquid-nitrogen temperature is in order, since a bias might be avoided or compensated for if some of these alternate hypotheses were correct.

(1) It was previously suggested that some calcium was present in $M1$ (Dowty and Lindsley, 1970), but this now seems unlikely, in view of the larger anomalies subsequently verified in the room temperature spectra, which definitely require another explanation. Also, X-ray refinements of synthetic hedenbergite (Veblen and Burnham, 1969) and $Fs_{85}Wo_{15}$ (Y. Ohashi, personal communication) gave no indication of calcium in $M1$.

(2) Systematic error in composition or contamination introduced in synthesis are not likely causes of the bias, because all effects of this type (of which we are aware) would lead to a bias in the opposite direction. Incomplete reaction at 20 kbar leads to the assemblage pyroxene plus fayalite plus silica, and the pyroxene is more calcic than the nominal composition of the run. The Mössbauer absorptions for iron in fayalite overlap with the pyroxene $M1$ doublet and not with $M2$. Therefore, if reaction were incomplete, we would expect a "double" enhancement of $M1$ at the expense of $M2$.

(3) Cause of the bias through differences in recoil-free fractions for the two sites would indicate

TABLE 6. Hyperfine Parameters (mm/sec) for Multi-Doublet Fits to Room Temperature Spectra of Synthetic Hedenbergite-Ferrosilite Pyroxenes

Fs Content	M1* (1) QS	(1) IS	(2) QS	(2) IS	(3) QS	(3) IS	(4) QS	(4) IS	M2 QS	M2 IS
50	--	--	--	--	--	--	2.222(2)**	1.188(2)**	--	--
60	--	--	2.762(1)	1.191(5)	2.497(7)	1.101(3)	2.185(6)	1.184(3)	1.833(8)	1.152(4)
70	--	--	2.729(6)	1.178(3)	2.431(6)	1.191(3)	2.069(9)	1.185(5)	1.787(6)	1.129(3)
75	2.686(3)	1.156(1)	2.642(1)	1.183(6)	2.289(1)	1.175(6)	2.047(2)	1.142(1)	1.740(6)	1.111(3)
80	2.738(5)	1.183(3)	2.512(3)	1.187(2)	2.119(7)	1.181(4)	--	--	1.719(3)	1.115(2)
85	2.690(4)	1.182(2)	2.442(4)	1.193(2)	2.101(7)	1.194(4)	--	--	1.754(3)	1.114(2)
87.5	2.616(10)	1.179(5)	2.343(13)	1.212(6)	2.0(1)	1.219(6)	--	--	1.811(3)	1.116(1)
90	2.619(3)	1.180(2)	2.295(5)	1.199(3)	--	--	--	--	1.852(3)	1.129(2)
98	2.488(3)**	1.179(1)**	--	--	--	--	--	--	1.910(3)**	1.125(2)**
100	2.490(5)**	1.182(3)**	--	--	--	--	--	--	1.906(4)**	1.130(2)**

*Divided as in Table 2.

**Values from Table 4.

QS is quadrupole splitting, IS is isomer shift. Values in parentheses represent estimated standard deviation from the least-squares fits, in terms of least units cited.

a larger thermal motion for $M1$ than for $M2$ iron, which would conflict with relative temperature factors measured by X-ray diffraction. Our measurements for orthoferrosilite, the only composition for which the recoil-free fractions can be compared unambiguously, indicate no difference between the two sites within the error of measurement (Tables 4 and 9).

(4) Some bias might be expected because of saturation effect, *i.e.*, the fact that the increase in area of a peak drops off nonlinearly with increasing iron concentration, when the concentration is relatively high. This would effectively reduce the area of $M1$ more than $M2$, because the $M1$ iron concentration is always greater (except for Fs_{100}). However, this effect should be related to total iron content in the absorber, and there seems to be no correlation of the anomaly with iron concentration in our absorbers. Absorbers of two compositions, $Fs_{60}Wo_{40}$ and $Fs_{70}Wo_{30}$, were prepared with especially low iron concentrations, and were run with the palladium source, as a test for saturation effects and for any effects of the use of the chromium source in the original spectra (the Cr source has a relatively broad line). The anomaly was not significantly reduced for these spectra. (These spectra are marked with an asterisk in Table 9).

We conclude that the bias in liquid-nitrogen temperature spectra probably is caused by the same phenomenon as the bias in room temperature spectra, and is therefore essentially unavoidable in measurements of calcium-bearing pyroxenes. The implications of this and another possible cause of bias will be discussed in the concluding section.

Quadrupole Splitting

The existence of two peaks in the Mössbauer spectrum for each site is due to a non-cubic charge distribution around the iron nucleus, and the separation of the two peaks, quadrupole splitting, is dependent on the degree of distortion of the charge from cubic symmetry. The quadrupole splitting can in principle be calculated if the crystal structure is known, but the computations are exceedingly complex for low site symmetry, and there are several factors entering into the calculation which are not perfectly known and are difficult to measure independently. It is not always possible, therefore, to attain absolute accuracy. If some simplifying assumptions are made about the geometry of the site, however, and if we are satisfied with results which are only qualitative, or at most, accurate in a relative sense, then some relationships may be developed which apply to a significant range of site configurations. Ingalls (1964) has derived a set of relationships for distorted octahedral sites which we will attempt to use to interpret relative variations in the quadrupole splitting of synthetic hedenbergite-ferrosilite pyroxenes.

TABLE 7. Widths (mm/sec) for Multi-Doublet Fits to Room Temperature Spectra of Synthetic Hedenbergite-Ferrosilite Pyroxenes

Fs Content	M1* (1)	(2)	(3)	(4)	M2
50	–	–	–	0.296**	–
60	–	0.127(10)	0.308(7)	.302(3)	0.278(7)
70	–	.255(3)	.309(3)	.278(3)	.296(3)
75	0.251(3)	.259(6)	.326(3)	.261(3)	.272(3)
80	.197(2)	.287(3)	.309(3)	–	.282(3)
85	.208(2)	.218(3)	.271(3)	–	.305(3)
87.5	.269(3)	.318(3)	.287(3)	–	.291(3)
90	.237(2)	.313(3)	–	–	.291(3)
98	.299**	–	–	–	.285**
100	.280**	–	–	–	.246**

*Divided as in Table 2.

**Average from Table 4.

Widths of the two peaks of a doublet constrained to be equal, except for values from Table 4. Figures in parentheses represent estimated standard deviation from the least-squares fits, in terms of least units cited.

TABLE 8. Data Collection Information and Chi-Square Values for Liquid-Nitrogen Temperature Spectra of Synthetic Hedenbergite-Ferrosilite Pyroxenes

Fs Content	Iron conc. mg/cm	background counts x 10^6	Chi-square Lorentz.	Gauss.
50 (1)	3.7	0.68	626	539
(2)	3.7	.58	1183	1145
(3)	3.7	.25	243	232
60 (1)	4.6	.78	710	372
(2)	1.5	2.18	787	416
70 (1)	3.8	.86	521	262
(2)	3.8	.78	480	283
(3)	1.7	1.66	652	409
75 (1)	7.0	.79	464	259
(2)	7.0	.36	632	383
80 (1)	7.3	.66	433	260
(2)	7.3	.68	786	517
85 (1)	6.7	.68	734	414
87.5 (1)	2.6	1.27	309	235
(2)	2.6	1.56	388	244
90 (1)	8.7	1.29	535	302
98 (1)	7.9	.57	436	385
(2)	7.9	.36	504	428
100 (1)	3.2	.43	432	360
(2)	3.2	1.18	242	215
(3)	3.2	.65	382	320

TABLE 9. Area Ratios and Mössbauer Parameters (mm/sec) for Fits to Liquid-Nitrogen Temperature Spectra of Synthetic Hedenbergite-Ferrosilite Pyroxenes

Fs Content	M2 area			M1				M2			
						Widths				Widths	
	Expected	Lorentz.	Gauss.	QS	IS	L	H	QS	IS	L	H
50 (1)	0.0	-	-	2.735(2)	1.300(2)	0.446(5)	0.452(4)	-	-	-	-
(2)	0.0	-	-	2.764(2)	1.308(2)	.409(6)	.377(4)	-	-	-	-
(3)*	0.0	-	-	2.778(3)	1.306(2)	.327(5)	.314(6)	-	-	-	-
60 (1)	0.167	0.184(12)	0.214(4)	2.873(2)	1.309(2)	.460(4)	.425(4)	1.905(6)	1.270(3)	0.314(8)	0.454(9)
(2)*	.167	.189(7)	.237(3)	2.876(2)	1.301(1)	.374(4)	.379(4)	1.942(6)	1.241(3)	.313(7)	.400(6)
70 (1)	.286	.308(8)	.323(3)	2.963(3)	1.300(2)	.416(6)	.421(5)	1.871(6)	1.234(3)	.381(9)	.425(6)
(2)	.286	.302(9)	.341(6)	2.970(3)	1.297(2)	.441(6)	.423(5)	1.884(6)	1.242(3)	.355(6)	.472(7)
(3)*	.286	.310(4)	.348(3)	2.956(2)	1.299(2)	.370(4)	.384(4)	1.862(4)	1.222(2)	.341(5)	.376(5)
75 (1)	.333	.381(5)	.385(3)	2.987(4)	1.288(2)	.534(7)	.526(6)	1.836(6)	1.217(3)	.530(10)	.536(7)
(2)	.333	.342(9)	.378(4)	2.990(2)	1.295(2)	.459(6)	.454(6)	1.832(4)	1.232(2)	.369(5)	.478(6)
80 (1)	.375	.396(7)	.420(3)	3.018(3)	1.291(2)	.481(6)	.455(5)	1.810(4)	1.222(3)	.426(6)	.512(8)
(2)	.375	.383(5)	.415(3)	3.024(2)	1.294(1)	.436(5)	.430(4)	1.801(3)	1.225(2)	.384(5)	.441(5)
85 (1)	.412	.438(10)	.455(4)	3.004(2)	1.285(2)	.458(5)	.448(5)	1.805(3)	1.221(2)	.412(5)	.504(6)
87.5 (1)	.429	.451(14)	.444(4)	3.065(3)	1.305(2)	.382(6)	.391(5)	1.914(4)	1.251(2)	.399(5)	.507(7)
(2)	.429	.442(7)	.438(4)	3.050(4)	1.300(2)	.414(6)	.414(6)	1.907(5)	1.243(3)	.400(5)	.525(7)
90 (1)	.444	.505(12)	.471(3)	3.068(3)	1.289(2)	.453(6)	.446(4)	1.966(3)	1.236(2)	.451(6)	.512(6)
98 (1)	.490	.505(8)	.507(3)	3.102(2)	1.297(2)	.361(5)	.367(5)	2.005(2)	1.254(2)	.357(4)	.412(6)
(2)	.490	.486(7)	.523(3)	3.147(3)	1.300(2)	.400(5)	.401(6)	2.020(3)	1.259(2)	.343(5)	.422(6)
100 (1)	.500	.496(13)	.486(3)	3.130(2)	1.297(2)	.337(6)	.332(4)	2.000(2)	1.258(2)	.334(5)	.372(5)
(2)	.500	.495(14)	.497(3)	3.140(2)	1.309(2)	.322(6)	.320(5)	2.004(2)	1.273(2)	.322(5)	.349(4)
(3)	.500	.497(8)	.540(5)	3.177(4)	1.304(2)	.361(5)	.369(6)	2.023(3)	1.261(2)	.331(6)	.406(7)

*These spectra were taken with a palladium source, the others with a chromium source.
Quadrupole splitting (QS), isomer shift (IS) and full widths at half height (low and high velocity) are from partially Gaussian fits. Figures in parentheses represent estimated standard deviation from each least-squares fit, in terms of the least unit cited.

In Ingalls' crystal-field model, the quadrupole splitting, ΔE, for ferrous iron in near-octahedral coordination is given by

$$\Delta E = \Delta E_0 \alpha^2 F(\Delta_1, \Delta_2, \lambda_0, \alpha^2, T) \qquad (2)$$

The heart of the model is the "reduction function" F, whose value is calculated by perturbation theory. ΔE_0 is the maximum possible value of quadrupole splitting,[4] α^2 is a covalency factor which has a value of 1.0 in perfectly ionic sites and is reduced for more covalent bonding, λ_o is a spin-orbit constant, T is the absolute temperature, and Δ_1 and Δ_2 are the two lowest splittings of the crystal-field levels, as shown in Figure 2. In general, the values of Δ_1 and Δ_2 may be thought of as increasing with the distortion of the coordination from perfect octahedral symmetry.

Curves of the reduction function F versus a distortion parameter, $\Delta/\lambda_o\alpha^2$, are drawn (Fig. 3) for the special case $\Delta = \Delta_1 = \Delta_2$ (the tetragonal case in Figure 2). This is the simplest case of distortion even of those treated by Ingalls, who also described orthorhombic distortion. In silicates, iron-site symmetries are commonly monoclinic (as in $C2/c$ pyroxenes) or triclinic (as in orthopyroxenes). Thus for many applications, the model in this form is an approximation at best. However, the orthorhombic part of the distortion is expected (Gibb, 1968) to be subsidiary to the axial part (tetragonal in this treatment), and contributions from distortion of symmetry lower than orthorhombic should be even less important.

Mainly for simplicity, we will analyze the quadrupole splitting as if the distortion of the iron sites in the hedenbergite-ferrosilite series can be uniquely correlated with the distortion parameter shown in Figure 3, at least with respect to relative variations within the series. We will show that this simplified approach yields an interpretation of quadrupole splitting variation in the series which is essentially complete and consistent with all observations. In view of the limitations of the model with respect to the symmetry of the sites, and our limited information about the actual configurations of the sites, part of our apparent success might well be fortuitous. Application of the model to other systems is not

[4] ΔE_0 for ferrous iron is approximately 5.6 mm/sec, for the formulation given here (Ingalls, 1964).

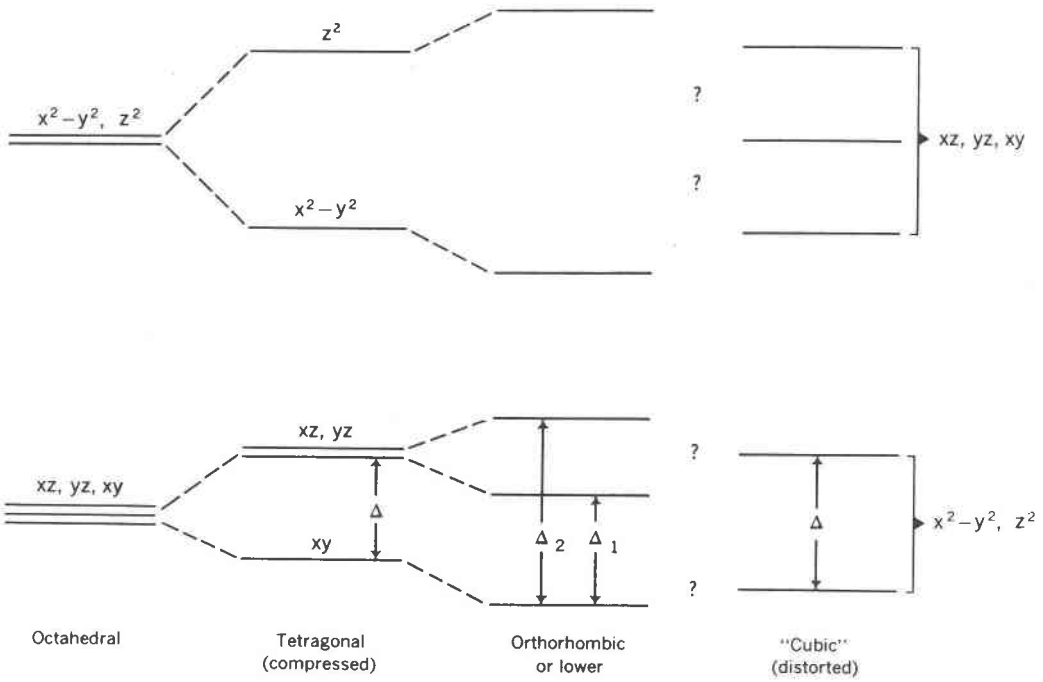

FIG. 2. Crystal field levels for various types of six and eight coordination showing the splitting of the lowest levels, Δ, or Δ_1 and Δ_2.

necessarily expected to be as straightforward, nor the results to be as consistent. Nevertheless, the usefulness of the model in the form used here should be evident.

The use of at least part of the Ingalls model has been suggested before in the mineralogical literature. For example, Bancroft, Maddock, and Burns (1967) pointed out that the quadrupole splitting of iron sites in many silicates is inversely correlated with the distortion of the coordination polyhedron. Our model differs from previous ones by suggesting that some iron sites may lie on the part of the quadrupole splitting curves with positive slopes, and in more systematically using the temperature dependence of the quadrupole splitting relationships.

We might add that Gibb (1968) has extended the valence-term part of the model to several other types of iron configurations, including high-spin tetrahedral and low-spin octahedral ferrous iron coordination, and low-spin octahedral ferric iron. Unfortunately, the lattice term, which we can usually expect to be important in structurally complex minerals, was not included in his calculations.

Explanation of the Model

The function F may be thought of as the sum of two terms, the lattice term and the valence term. The *lattice term* arises from the deviation from cubic symmetry of the surroundings of the iron atom, particularly the coordination polyhedron. It increases approximately linearly with the distortion parameter, $\Delta/\lambda_0\alpha^2$. The *valence term* arises from asymmetry of the electronic charge on the iron atom itself. Since the filled inner electron shells all have near-spherical symmetry, only the outermost, or valence shell, can contribute substantially to the quadrupole splitting. In iron, the incomplete part of the valence shell is composed of the five *d* orbitals. When each of the *d* orbitals is equally occupied by electrons, this shell is also spherically symmetric. Thus, in ferric iron, which has five *d* electrons, each orbital contains one electron. Thus the valence term is nonexistent and the quadrupole splitting is given by the lattice term only. Ferrous iron, however, has six *d* electrons, one extra. In the free ion, this extra electron spends its time uniformly among the five orbitals, since they are equally favorable energetically (degenerate). The transition time of the electron among the orbitals is sufficiently short that the time average of its distribution is spherically symmetric. In perfect octahedral coordination, three of the orbitals (the t_{2g} set) are more favorable than the other two, so the electron spends its time among these three. However, these three orbitals together are also spherically symmetric, so

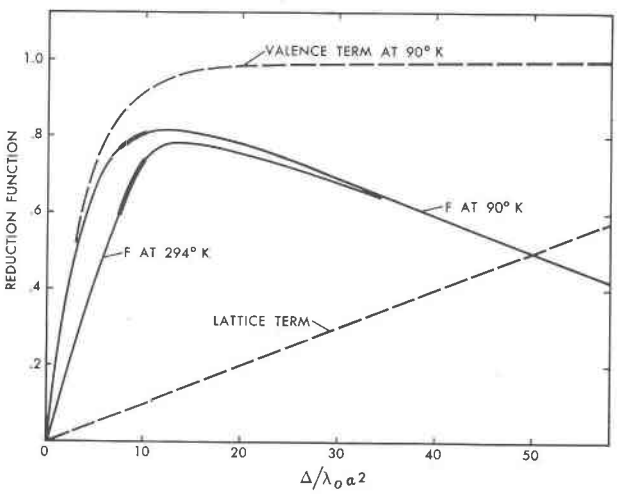

FIG. 3. Relation of the reduction function F, to distortion from perfect octahedral coordination, $\Delta/\lambda_o\alpha^2$. Quadrupole splitting is approximately 5.6 mm/sec times F times the covalency factor, α^2. The reduction function (solid lines) is the sum of the valence and lattice terms (dashed lines); the lattice term is shown here with sign reversed. The darkened segments are intended to represent the variation with composition of a single next-nearest-neighbor configuration for the $M1$ site, for example, any of numbers 1 through 4 in Figure 5. After Ingalls (1964).

that for both the free ion and perfect octahedral coordination, the quadrupole splitting is zero (although perfect octahedral coordination is seldom expected to exist for ferrous iron coordination, because of the Jahn-Teller effect). If the coordination distorts slightly from octahedral symmetry, one of the lower d orbitals becomes stabilized relative to the other two, and the electron spends most of its time in this orbital to produce a very strongly asymmetric charge distribution. Thus the valence term increases very rapidly with distortion to a maximum value corresponding to unique occupancy of the lowest energy orbital by the sixth d electron.

The lattice term is sensitive to temperature only insofar as the locations of other atoms relative to the iron nucleus change with temperature. Normally such changes are rather slight. The valence term can be quite sensitive to temperature because the distribution of electrons among different energy levels is temperature dependent and given by a Boltzman function. As thermal energy is infused into the atom, the sixth d electron can spend more time in higher energy orbitals to produce a more symmetric charge distribution and a lower value for the valence term. As the separation between the levels increases with distortion, however, higher temperature becomes inadequate to boost the electron to the next highest level. Therefore, the difference in quadrupole splitting between two given temperatures tends to decrease with increasing distortion, after reaching an initial maximum.

The quadrupole splitting, and each of the terms, may be positive or negative. The sign is not usually determinate from powder Mössbauer spectra alone, but the particular geometry of the d-orbitals relative to the crystal field requires that the signs of the lattice and valence terms be opposite to one another. The extra d electron naturally disposes itself in such a way as to counteract the potential of the surrounding atoms. To obtain the absolute value of F, shown by the doubly sloped curves in Figure 3, the lattice term as plotted in Figure 3 is subtracted from the valence term. The quadrupole splitting is equal to the "maximum" quadrupole splitting, ΔE_0, multiplied by F and the covalency factor (Eq. 2).

The value of $\Delta/\lambda_o\alpha^2$ can in principle be estimated independently, but, in fact, very few data are presently available to do so. The value of λ_o has been calculated theoretically at about 100 cm^{-1} (Ingalls, 1964), but this is for the free ion. The value of α^2 can only be guessed at, and is probably in the neighborhood of 0.6 to 0.8 for iron in silicates. The values of Δ_1 and Δ_2 can be obtained from optical spectra, but although a few optical measurements on pyroxenes have in fact been made, these can hardly be regarded as definitive with respect to establishing Δ_1 and Δ_2, and no measurements are available for the hedenbergite-ferrosilite series specifically (Burns, 1970, does give a spectrum of a natural hedenbergite). It will be necessary to take a qualitative approach in the present case, "fitting" the quadrupole-splitting data to the model curves.

The M1 site

The question arises whether the $M1$ site is associated with a positive or negative slope of the F curves (Fig. 3). We note that the $M1$ site is very little distorted in any pyroxene. Burns (1970) has inferred that Δ_1 and Δ_2 are probably less than 100 cm^{-1} in orthopyroxenes. If this is correct, $M1$ would fall in the region of positive slope, close to the zero point. The average deviation of the 6 $M1$–O bond lengths from the mean $M1$–O bond length, which is an index of distortion, is 0.027 Å in hedenbergite (data from Veblen and Burnham, 1969), whereas it varies from 0.040 to 0.048 in the orthopyroxene

series (data from Burnham, 1966; Morimoto and Koto, 1969). Quadrupole splitting increases a great deal between hedenbergite and orthoferrosilite (Fig. 4), which would appear to confirm that $M1$ lies on the part of the F curves with positive slope. Indeed, the magnitude of this difference in quadrupole splitting compared with the relatively small change in distortion seems to be more consistent with the positive-slope region, which is much steeper than the other part. Moreover the assumption that the $M1$ site is associated with the positive slope permits further rationalizations of the behavior of the doublets due to various next-nearest-neighbor configurations (see below) whereas these would not be possible if $M1$ were on the other part of the curves.

In Figure 4, the quadrupole splitting of $M1$ from two-doublet (one $M1$ doublet) fits is shown. There is a fairly smooth trend at both temperatures, although the quadrupole splitting at room temperature seems to reach a maximum in the middle of the series. When the multiple-doublet fits for the room temperature spectra are considered, a rather different picture emerges (Fig. 5). The trend for each of the next-nearest-neighbor configurations is in the opposite sense to the overall trend, indicating that the environment around iron becomes slightly more distorted as total calcium content is increased.

The apparent peak locations for the two-doublet fits do not correspond to the weighted mean of the locations of the various next-nearest-neighbor peaks, as a comparison of the data in Tables 4 and 6 shows. Rather, the peaks for the two-doublet fits are very close to the strongest of the next-nearest-neighbor peaks, or between the two strongest peaks—weaker next-nearest-neighbor peaks seem to have little influence. Thus, given the trends for the individual configurations shown in Figure 5, and the varying populations of each of these, it may be seen how the apparent quadrupole splitting of $M1$ from two-doublet fits to room temperature spectra could show a maximum in the middle of the series, as in Figure 4.

At liquid-nitrogen temperature, the doublets for the various $M1$ configurations are evidently closer to each other than at room temperature. In Figure 5, this would have the effect of drawing together the points for each composition and flattening the trend for each configuration. This also may be explained by a detailed consideration of the model curves in Figure 3. Note that the curves for the two temperatures have different slopes in the region just on the low-distortion side of the maximum; this is shown by the darkened segments representing a given small range of distortion. Each type of next-nearest-neighbor configuration could be represented by such a segment, with the less calcic composition being the lower (less distorted) end.

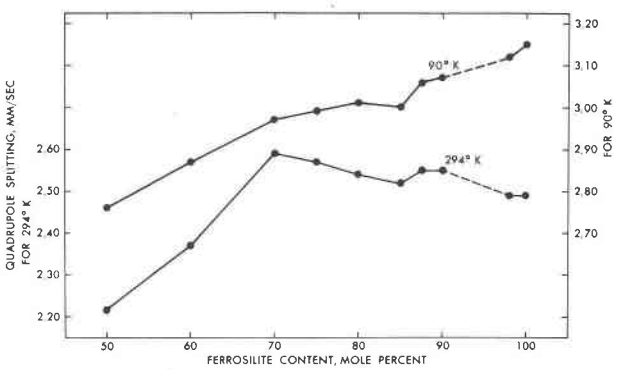

FIG. 4. Quadrupole splitting of the $M1$ site from two-doublet fits (one $M1$ doublet).

It should perhaps be emphasized that although the quadrupole splitting of the $M1$ configurations changes a good deal with composition, and the configurations are rather distinct from one another, only relatively small differences in distortion are indicated. The large differences in quadrupole splitting are due to the steep slope of the F curves in the low-distortion region. The differences in distortion between next-nearest-neighbor configurations are most probably caused by slight positional adjustments of the oxygen atoms coordinating $M1$ in response to the

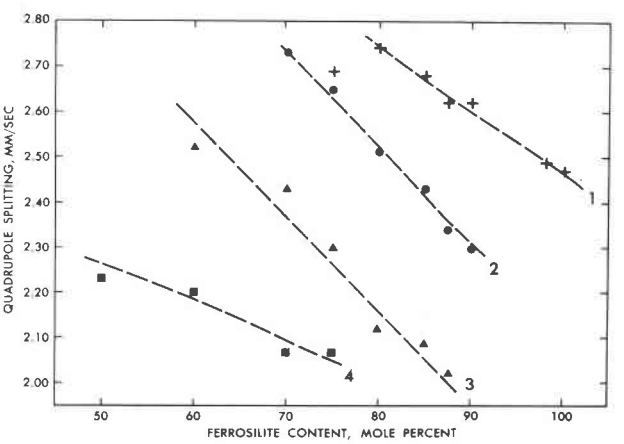

FIG. 5. Quadrupole splitting of the $M1$ site at room temperature from multi-doublet fits (up to four $M1$ doublets). Numbers 1 through 4 correspond to the next-nearest-neighbor configurations in Table 2.

differing occupancies of the three adjacent $M2$ sites. Positional disorder of the oxygen atoms in clinopyroxenes with intermediate calcium content has been indicated by X-ray refinements (Takeda, in preparation). The changes in quadrupole splitting of each type of next-nearest-neighbor configuration with composition evidently result from the pervasive effects of the calcium/iron ratio throughout the structure. The slopes for some of the configurations in Figure 5 are surprisingly large in comparison with the changes in quadrupole splitting due to changes in next-nearest-neighbor populations in the same series, and in other mineral series (*e.g.*, olivines; Bancroft, Maddock, and Burns, 1967). This might be considered anomalous, but the trends seem susceptible to rationalization on the basis of the model curves (above). The absence of comparable trends in other minerals possibly indicates that the $M1$ site in our pyroxenes is almost unique in its low distortion and consequent high susceptibility to slight structural changes.

The M2 site

The few optical data indicate that at least one of the Δ's for $M2$ in pyroxenes is large; the value of 3000 cm^{-1} determined for orthopyroxenes (Bancroft and Burns, 1967b; White and Keester, 1967) is probably exceeded in clinopyroxenes. X-ray results also indicate that $M2$ is much more distorted than $M1$, even in ferrosilite, where the coordination of $M2$ is six. This becomes more pronounced in hedenbergite where the $M2$ site contains calcium in a distorted eight-coordination. The quadrupole splitting of $M2$ shows relatively slight temperature dependence. These considerations leave no doubt that $M2$ falls well out on the F curves in Figure 3 where the slopes are negative. To the extent that the distortion of the coordination is adequately described by the crystal-field model for octahedral coordination, the quadrupole splitting of $M2$ would tend to decrease only moderately for a large increase in distortion.

As pointed out before, an $M2$ cation is not approached as closely by other $M2$ cations as is an $M1$ cation. Since the $M2$ site is also in a region of distortion in which the quadrupole splitting is much less sensitive to changes in the environment, the $M2$ site is probably adequately represented by one doublet. However, overlap of $M1$ peaks on the $M2$ doublet does appear to have an influence on the apparent locations of the $M2$ peaks. Whereas with the two-doublet fits, the quadrupole splitting of $M2$ appeared to be temperature dependent in calcium-poor compositions but not in calcium-rich compositions, the multidoublet fits indicate that the temperature dependence is small, but more or less the same for all compositions (Fig. 6).

The changes in quadrupole splitting of the $M2$ site through the series are undoubtedly related to the way in which the coordination of this site changes from six around iron in ferrosilite to eight around calcium in hedenbergite. The actual atomic positional changes of oxygen atoms surrounding $M2$ have been described for a partial series of low- to high-calcium pyroxenes by Takeda (1972; in preparation). The changes in coordination are chiefly related to displacements of the O3 oxygen atoms.

The trends shown in Figure 6 seem inconsistent with the idea that the iron cation, which is small in relation to calcium, maintains its own type of coordination in the series (as suggested for iron and magnesium in pigeonite by Morimoto and Tokonami, 1969). If this were true, we would expect a more nearly linear trend, and probably less abrupt change, especially at the low-calcium end. The fact that there is a very pronounced change in quadrupole splitting almost as soon as calcium enters the structure, and the fact that there are minima in the curves, suggests that the coordination of Fe changes significantly even at low concentrations of calcium. The same conclusion has been reached by Takeda (1972; in preparation) on the basis of thermal parameters of the oxygen atoms.

In the more calcic pyroxenes of the series we may assume that the coordination of iron atoms is similar to that described by Takeda (1972; in preparation) for iron and magnesium in subcalcic augites. This is a four-plus-four coordination, in which the cavity, formed by eight oxygen atoms, is similar to that in which the calcium atom is found, but the iron or magnesium atom is very much to one side so that the bond distances are normal to only four of the oxygen atoms.

One of the most interesting aspects of the quadrupole spliting curves for $M2$ in Figure 6 is the fact that they bear a pronounced resemblance to the clinopyroxene miscibility gap (as it is known in more magnesian compositions) turned upside down. The slopes of the quadrupole splitting "solvi" are steep on the pigeonite side and more gradual on the $C2/c$ side, as we expect the real solvi to be, and the minimum of the curve also coincides approximately with the change in symmetry observed in X-ray

photographs. This might be regarded as an illustration of the crystal-chemical basis for the real miscibility gap. The minimum of quadrupole splitting probably represents maximum distortion, and therefore greatest potential energy of the structure in the vicinity of the iron atoms at this composition. Other factors being nearly equal, this might cause this composition to be unstable with respect to compositions both more and less calcic. The quadrupole splitting model is not technically applicable to the type of iron coordination found in the more calcic pyroxenes (closer to eight than six coordination) but the very fact that the trend in quadrupole splitting corresponds to the phase relations suggests that it is at least qualitatively useful in this case.

Isomer Shift

With the correct assignment of the *M*2 doublet inside the *M*1 doublet, the isomer shift of *M*1 is 0.04 to 0.08 mm/sec larger than that of *M*2. The difference between room and liquid-nitrogen temperatures of about 0.11 mm/sec for both sites may be ascribed to a thermal (second-order Doppler) shift.

In the room temperature spectra, there is no definite evidence that the isomer shifts of the various *M*1 doublets (Table 6) are different from each other. The total error is somewhat large for these measurements, probably because of the approximations made in the fitting and the near-marginal amount of information in the data in relation to the number of fitted parameters.

For the *M*2 doublet, the isomer shift seems to be slightly lower in the middle of the series at both temperatures. If this is real, it may possibly be related to the differences in the nature of the bonding expected as the coordination of *M*2 iron changes through the series from six to four-plus-four. In the four-plus-four coordination, the anisotropic nature of the bonds (all strong bonds on one side of the iron atom) implies a greater degree of covalency. The increase in isomer shift at the calcic end of the series is not readily explicable.

Line Widths and Symmetry of the Doublets

For a number of reasons, line widths reported are not good estimates of "intrinsic" line widths. First, there are instrumental effects, which are apparent in the different line widths obtained for duplicate spectra of the same absorber at liquid-nitrogen temperature (Table 9). These are probably due primarily to temperature variation and cryostat vibration and are expected to be less at room temperature. Fortunately, such variation seems to have little effect on area ratios or hyperfine parameters.

Second, the two-doublet fits apparently are not the best model for the spectra, and the meaning of line widths for these spectra is therefore questionable.

Third, some broadening may be caused by compositional inhomogeneity. This type of broadening is difficult to isolate from that due to next-nearest-neighbor effects, since the two compositions which are least likely to be inhomogeneous, Fs_{50} and Fs_{100}, also do not suffer from next-nearest-neighbor effects. These compositions give reasonably narrow lines (Tables 4 and 9).

For the multi-doublet, room-temperature fits, widths are also reasonably small (see Table 7), but precision is poor and constraints were used, so that these measurements are probably not meaningful with respect to detection of composition broadening.

One apparent trend which does emerge is a tendency for the width of the high velocity peak of the *M*2 doublet at liquid-nitrogen temperature to be larger than that of the low-velocity peak (Table 9). If this is not due to partial overlap of *M*1 absorption, relaxation effects are probably indicated, because the height of the high-velocity peak is concomitantly reduced, so that the areas of the two peaks are not significantly different. Shenoy, Kalvius, and Hafner (1969) found that spin-lattice relaxation effects in the orthopyroxene series increase with decreasing iron content. In our case also, the effect seems to

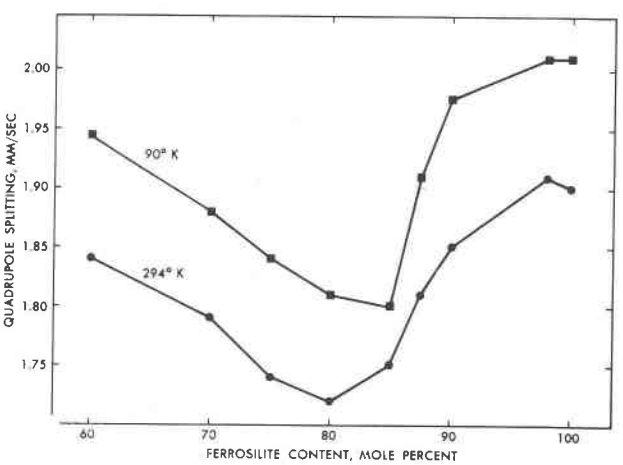

FIG. 6. Quadrupole splitting of the *M*2 site at room temperature from multi-doublet fits, and at liquid-nitrogen temperature from two-doublet fits.

increase with decreasing content of iron in $M2$, although we note that $M1$ is always fully occupied by iron. We attempted fits of the room temperature spectra with the constraints released for the $M2$ doublet only, to find out if the asymmetry is less than at low temperature, as predicted for relaxation. The widths and heights of the two $M2$ peaks did not appear to be significantly different, and the values of chi-square were not significantly reduced in these fits, but again, the comparison may not be meaningful because of the poor resolution.

If the interpretation of asymmetry as due to relaxation is correct, the method of estimating site occupancies by using peak heights alone (Virgo and Hafner, 1969) is not strictly valid in pyroxenes with low concentrations of iron in $M2$; by this method, the area of the high-velocity peak of $M2$ would be underestimated. However, the bias thus produced would be in the opposite sense to that produced by the splitting of the $M1$ absorption.

Application to Natural Pyroxenes and Other Minerals

Accuracy of room temperature measurements of clinopyroxenes

The use of room temperature spectra for determining iron-site occupancy in orthopyroxenes was previously shown by Virgo and Hafner (1968) to be inferior to the use of liquid-nitrogen temperature spectra. This follows solely from the poorer resolution of $M1$ from $M2$ doublets at room temperature. The same applies to clinopyroxenes, in which the anomalies caused by different $M1$ configurations give further reason for not using room temperature spectra. We have apparently had some success in fitting multiple $M1$ doublets to our spectra, but the simple compositions enabled us to predict the population of the different $M1$ configurations. Such predictions would be impossible in natural clinopyroxenes, because the compositions are much more complex and the $M1$–$M2$ iron distribution is not known.

Accuracy of liquid-nitrogen temperature measurements

Resolution of $M1$ from $M2$ is much better at liquid-nitrogen temperature, but two-doublet fits still overestimate the $M2$ area in our calcium-bearing pyroxenes (Fig. 7). Since we had no success in fitting multiple $M1$ doublets in our simple compositions, it is unlikely that such fits would be possible in natural clinopyroxenes, and the two-doublet fits probably must be accepted as the best estimates of the iron site distribution. If we are to use these estimates, some correction is necessary. Our measurements (Fig. 7) provide tentative values for correction factors, but it is quite likely that these would not be applicable to more complex natural clinopyroxenes.

In the following subsections, we apply the experimental results and hypotheses discussed above to specific types of pyroxenes. If the hypotheses proposed in this work are accepted, it is evident that a certain amount of reinterpretation of previous work is necessary.

Augites and pigeonites

In common Mg–Fe–Ca pyroxenes, an additional source of bias may be present which is distinct from that caused by next-nearest-neighbor influence. Augites and pigeonites and also orthopyroxenes commonly consist of intergrowths of one with another, as a result of exsolution from high-temperature precursors. Since the difference in composition of the exsolved phases is chiefly in calcium content, our results permit the Mössbauer parameters of the members of these intergrowths to be predicted to a first approximation, at least for very iron-rich pyroxenes. We discuss only liquid-nitrogen spectra since, as explained above, room-temperature data are not likely to be useful at all for purposes of determining site occupancies.

The quadrupole splitting of $M2$ shows some variation with calcium content, but since the shape of the curve for $M2$ quadrupole splitting *vs* temperature resembles the clinopyroxenes solvus, the two members of a pigeonite-augite intergrowth and possibly also an orthopyroxene-augite intergrowth will have $M2$ doublets which are fairly closely superposed. On the other hand, the variation of the quadrupole splitting of $M1$ is larger than that of $M2$ and not related to the pattern of exsolution. Thus the $M1$ doublets of the two pyroxenes in an intergrowth may be rather dissimilar. If only one doublet is fitted for $M1$ in such an intergrowth, the result may produce a bias in the same way, and in the same direction, as next-nearest-neighbor influence.

High-calcium pyroxenes (augites) from lunar rocks have been reported to be more completely ordered with respect to Fe–Mg site distribution than coexisting low-calcium pyroxenes, or than low-calcium pyroxenes in rocks with presumably similar cooling histories (Hafner and Virgo, 1970; Hafner

et al, 1971). At least part of this apparently greater order is probably due to overestimation of *M*2 iron occupancy because of either or both kinds of bias. Certainly, the apparent excess of *M*2 cations (iron plus calcium) which has been indicated from Mössbauer measurement of some specimens of lunar high-calcium iron-rich pyroxenes (Hafner *et al,* 1971) may be attributed to this bias (Dowty *et al,* 1972).

Diopside-hedenbergite series

In a study of natural diopside-hedenbergite pyroxenes, Bancroft, Williams, and Burns (1971) noted that in one specimen with slightly less than the maximum amount of calcium, there was evidence not only for doublets representing *M*1 and a slight amount of *M*2 iron, but a third weak doublet which they could not identify conclusively. The third doublet could well be due to next-nearest-neighbor configuration type 3, in the nomenclature of Table 2. (Pure diopside-hedenbergite should have only a type 4 doublet, assuming iron and magnesium are essentially interchangeable.)

Omphacites

Omphacites are sodic pyroxenes which usually have space group *P*2 and four symmetrically distinct types of *M*1 sites. Bancroft, Williams, and Essene (1969) found evidence for four different ferrous doublets in natural omphacites and inferred that ferrous iron was disordered over all four *M*1 sites. The present results suggest that some of these doublets may have been due to next-nearest-neighbor effects, and that ferrous iron may be in only two of the *M*1 sites, as previously inferred from X-ray diffraction data (Clark and Papike, 1968).

Other minerals

In iron sites in silicates there seems to be a general negative correlation of quadrupole splitting with distortion (Bancroft, Maddock, and Burns, 1967). This suggests that most of these sites lie in a region of distortion in which next-nearest-neighbor influences would not be likely to cause the kind of splitting found in the *M*1 site of clinopyroxenes. Nevertheless, the possibility of splitting of this kind should not be overlooked; the type of low-distortion site which is likely to be affected by next-nearest-neighbor influences will probably show a relatively high dependence of quadrupole splitting or temperature.

Another class of minerals which we may immediately suspect as being susceptible to this effect is the calcic and alkali amphiboles, because of the many structural and chemical similarities between pyroxenes and amphiboles.

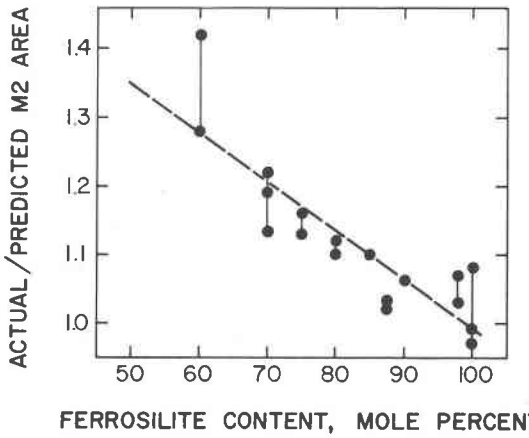

FIG. 7. Discrepancy in area ratios of liquid-nitrogen temperature spectra, two-doublet, partially Gaussian fits. The dashed line is a least-squares fit to the data.

Acknowledgments

The Mössbauer equipment for this study was furnished through the courtesy of the National Bureau of Standards, U.S. Department of Commerce, Gaithersburg, Maryland. We thank J. J. Spijkerman, P. A. Pella, J. C. Travis, N. Debye, and J. R. DeVoe of that laboratory for their personal assistance at various stages in the project. Charles W. Burnham provided helpful criticism and guidance, and we thank him and Y. Ohashi for the use of their unpublished results. J. C. Travis also provided guidance on technical points and inspiration for the use of non-Lorentzian line shapes. The final partially Gaussian line shape was arrived at through the comments of W. A. Dollase. H. T. Evans kindly indexed and refined the Guinier powder data of several specimens. The manuscript has been greatly improved by the criticism of S. S. Hafner, and we thank him for correction on several technical points. The writers bear sole responsibility for interpretations and conclusions in this paper.

References

BANCROFT, G. M., AND R. G. BURNS (1967a) Distribution of iron cations in a volcanic pigeonite by Mössbauer spectroscopy. *Earth Planet. Sci. Lett.* **3,** 125–127.

———, AND ——— (1967b) Interpretation of the electronic spectra of iron in pyroxenes. *Amer. Mineral.* **52,** 1278–1287.

———, A. G. MADDOCK, AND R. G. BURNS (1967) Applications of the Mössbauer effect to silicate mineralogy: I. Iron silicates of known crystal structure. *Geochim. Cosmochim. Acta,* **31,** 2219–1146.

———, P. G. L. WILLIAMS, AND E. J. ESSENE (1969) Mössbauer spectra of omphacites. *Mineral. Soc. Amer. Spec. Pap.* **2,** 59–65.

———, ———, AND R. G. BURNS (1971) Mössbauer spectra of minerals along the diopside-hedenbergite tie line, *Amer. Mineral.* **56,** 1617–1625.

BURNHAM, CHARLES W. (1966) Ferrosilite. *Carnegie Inst. Washington Year Book,* **65,** 285–290.

———, Y. Ohashi, S. S. Hafner and D. Virgo (1971) Cation distribution and atomic thermal vibrations in an iron-rich orthopyroxene. *Amer. Mineral.* **56,** 850–576.

BURNS, R. G. (1970) *Mineralogical Applications of Crystal Field Theory.* Cambridge University Press, Cambridge.

CHRISTIE, J. M., J. S. LALLY, A. M. HEUER, R. M. FISHER, D. T. GRIGGS, AND S. V. RADCLIFFE (1971) Comparative electron petrography of Apollo 11, Apollo 12, and terrestrial rocks. *Geochim. Cosmochim. Acta, Suppl. 2,* **1,** 69–89.

CLARK, J. R., AND J. J. PAPIKE (1968) Crystal-chemical characterization of omphacites. *Amer. Mineral.* **53,** 840–868.

———, M. ROSS, AND D. E. APPLEMAN (1971) Crystal chemistry of a lunar pigeonite. *Amer. Mineral.* **56,** 888–908.

DAVIDON, W. C. (1959) *Variable metric method for minimization.* Argonne National Laboratory, ANL **5990.**

DEVOE, J. R., Editor (1967) *NBS Technical Note 421.* U.S. Government Printing Office, Washington, D. C.

DOWTY, E., AND D. H. LINDSLEY (1970) Mössbauer spectroscopy of synthetic Ca-Fe pyroxenes. *Carnegie Inst. Washington Year Book,* **69,** 190–193.

———, M. ROSS, AND F. CUTTITTA (1972) Fe^{2+}-Mg site distribution in Apollo 12021 pyroxenes: Evidence for bias in Mössbauer measurements and relation of ordering to exsolution. *Proc. Third Lunar Sci. Conf., Geochim. Cosmochim. Acta, Suppl. 3,* **1,** 481–492.

DUNDON, R. W., AND S. S. HAFNER (1971) Cation disorder in shocked orthopyroxene. *Science,* **174,** 581–583.

———, AND D. H. LINDSLEY (1967) Mössbauer study of synthetic Ca-Fe clinopyroxenes. *Carnegie Inst. Washington Year Book,* **66,** 366–369.

GIBB, T. C. (1968) Estimation of ligand field parameters from Mössbauer spectra. *J. Chem. Soc.* (London), **1968A,** 1439–1444.

GHOSE, S. (1965) Mg^{2+}–Fe^{2+} order in an orthopyroxene, $Mg_{0.93}Fe_{1.07}Si_2O_6$. *Z. Kristallogr.* **122,** 81–99.

HAFNER, S. S., AND D. VIRGO (1970) Temperature-dependent cation distributions in lunar and terrestrial pyroxenes. *Proc. Apollo 11 Lunar Sci. Conf., Geochim. Cosmochim, Acta Suppl. 1,* Vol. **3,** 2183–2198.

———, ———, AND D. WARBURTON (1971) Cation distributions and cooling history of clinopyroxenes from Oceanus Procellarum. *Geochim. Cosmochim. Acta, Suppl. 2,* Vol. **1,** 91–108.

INGALLS, R. (1964) Electric-field gradient tensor in ferrous compounds. *Phys. Rev.* **133A,** 787–795.

LINDSLEY, D. H., AND J. L. MUNOZ (1969) Subsolidus relations along the join hedenbergite-ferrosilite. *Amer. J. Sci.* **267A,** 295–324.

MATSUI, Y., Y. MAEDA, AND Y. SYONO (1970) Mössbauer study of synthetic calcium-rich pyroxenes. *Geochem. J.* **4,** 15–26.

MORIMOTO, N., AND K. KOTO (1969) The crystal structure of orthoenstatite. *Z. Kristallogr.* **129,** 65–83.

———, AND M. TOKONAMI (1969) Domain structure of pigeonite and clinoenstatite. *Amer. Mineral.* **54,** 725–740.

POSENER, D. W. (1959) The shape of spectral lines: Tables of the Voigt profile. *Austr. J. Phys.* **12,** 184–196.

SAXENA, S. K., AND S. GHOSE (1970) Order-disorder and the activity-composition relation in a binary crystalline solution. I. Metamorphic orthopyroxene *Amer. Mineral.* **55,** 1219–1225.

———, AND ——— (1971) Mg^{2+}–Fe^{2+} order-disorder and the thermodynamics of the orthopyroxene crystalline solution. *Amer. Mineral.* **56,** 532–559.

SHENOY, G. K., G. M. KALVIUS, AND S. S. HAFNER (1969) Magnetic behavior of the $FeSiO_3$–$MgSiO_3$ orthopyroxene system from NGR in ^{57}Fe. *Jour. Appl. Phys.* **40,** 1314–1316.

SMYTH, J. R. (1969) Orthopyroxene-high-low clinopyroxene inversions. *Earth Planet. Sci. Lett.* **6,** 406.

TAKEDA, H. (1972) Structural studies of rim augite and core pigeonite from lunar rock 12052. *Earth Planet. Sci. Lett.* **15,** 65–71.

VEBLEN, D. R., AND C. W. BURNHAM (1969) The crystal structures of hedenbergite and ferrosalite. (abstr.) *Canad. Mineral.* **10,** 147.

VIRGO, D., AND S. S. HAFNER (1968) Re-evaluation of the cation distribution in orthopyroxenes by the Mossbauer effect. *Earth Planet. Sci. Lett.* **4,** 265–269.

———, AND ——— (1969) Fe^{2+}, Mg order-disorder in heated orthopyroxenes *Mineral. Soc. Amer. Spec. Pap.* **2,** 67–81.

———, AND ——— (1970) Fe^{2+}, Mg order-disorder in natural orthoyproxenes. *Amer. Mineral.* **55,** 201–223.

WHITE, W. B., AND K. L. KEESTER (1967) Selection rules and assignments for the spectra of ferrous iron in pyroxenes. *Amer. Mineral.* **52,** 1508–1514.

WILLIAMS, P. G. L., G. M. BANCROFT, M. G. BOWN, AND A. C. TURNOCK (1971) Anomalous Mössbauer spectra of *C2/c* clinopyroxenes. *Nature Phys. Sci.* **230,** 149–151.

Manuscript received, February 7, 1972; accepted for publication, May 3, 1973.